Reassessing the unifying hypothesis for hypercontractility caused by myosin mutations in hypertrophic cardiomyopathy

James Spudich, Neha Nandwani, Julien Robert-Paganin, Anne Houdusse, Kathleen Ruppel

The unifying hypothesis for hypercontractility caused by hypertrophic cardiomyopathy: Nine years later

James A. Spudich[1,*], Neha Nandwani[1], Julien Robert-Paganin[2], Anne Houdusse[2] and Kathleen M. Ruppel[1,3,*]

1. Department of Biochemistry, Stanford University School of Medicine, Stanford, California 94305, United States.
2. Structural Motility, Institut Curie, Paris Université Sciences et Lettres, Sorbonne Université, CNRS UMR144, F-75005 Paris, France.
3. Department of Pediatrics, Stanford University School of Medicine, Stanford, California 94305, United States.

[*]Correspondence: jspudich@stanford.edu or kmer@stanford.edu

Abstract

Human β-cardiac myosin exists in an ON-state where both myosin heads are accessible for interaction with actin (N_a) and an OFF-state where the heads are folded back onto their own coiled-coil tail and interacting with each other in an interacting heads motif (IHM). Hypertrophic cardiomyopathy (HCM) mutations in β-cardiac myosin cause hypercontractility of the heart. A unifying hypothesis was proposed nine years ago that the hypercontractility caused by myosin HCM mutations is primarily due to an increase in N_a rather than by increases in fundamental parameters of myosin function such as intrinsic force of the motor, its velocity of movement along actin, or its ATPase turnover rate, all of which impact power output. This unifying hypothesis is revisited in light of accumulated data measuring all these parameters and the recent availability of a 3.6 Å resolution structure of the human β-cardiac myosin IHM. Biochemical measurements show that nearly all myosin HCM mutations examined show an increase in N_a regardless of where they occur in the myosin head domain, consistent with the unifying hypothesis.

Introduction

Hypertrophic cardiomyopathy (HCM) is the most frequently occurring inherited cardiac disease and is an important cause of arrhythmias and heart failure. It is associated with mutations in genes encoding various sarcomeric proteins (Seidman and Seidman, 2001), but most mutations occur in either *MYH7* or *MYBPC3*, encoding β-cardiac myosin heavy chain and myosin binding protein-C (MyBP-C), respectively. Mutations in these two genes account for over 80% of patients with HCM for whom a genetic variant has been discovered, with about 40% of those occurring in *MYH7* and the remaining 60% occurring in *MYBPC3* (Alfares *et al.*, 2015). The mutations in *MYBPC3* primarily cause truncations of the protein, which leads to haploinsufficiency (Marston *et al.*, 2009; van Dijk *et al.*, 2009; Harris, Lyons and Bezold, 2011). HCM is common, affecting more than 1 in 500 to 1 in 200 individuals (Semsarian *et al.*, 2015; Virani *et al.*, 2020). It is characterized by left ventricular hypertrophy in the absence of predisposing conditions, and ultimately causes decreased volume of the left ventricular chamber and often obstruction of the aortic outflow tract during systole. The conventional view is that HCM mutations result in hyperdynamic cardiovascular physiology (hypercontractility) that is often seen as a supranormal ejection fraction (EF) on echocardiograms even before hypertrophy is manifest (Ho *et al.*, 2002, 2009; Captur *et al.*, 2014; Haland *et al.*, 2016), and therapies are aimed toward controlling the hyperactive physiology.

To understand the molecular basis of this mutation-induced hypercontractility, it is essential to reconstitute the functions of interest from purified proteins (Kawana, Spudich and Ruppel, 2022). In this regard, a major advance in the field was the establishment of a mammalian myosin expression system in the mouse myogenic cell line C2C12 (Srikakulam and Winkelmann, 2004; Liu, Srikakulam and Winkelmann, 2008; Resnicow *et al.*, 2010; Deacon *et al.*, 2012). In collaboration with the Leinwand laboratory at the University of Colorado at Boulder, the Spudich/Ruppel laboratory at Stanford established the expression of human β-cardiac myosin containing the relevant human ventricular light essential (ELC) and regulatory (RLC) light chains. The availability of a pure human β-cardiac myosin reconstituted with the relevant human cardiac ventricular light chains allowed the analysis of the effects of HCM mutations on the functions of interest that would contribute to the hypercontractile state.

The prevailing view at the time was that HCM-causing mutations in the human β-cardiac myosin gene *MYH7* caused hypercontractility of the heart by increasing one or more of the fundamental parameters of the myosin, which are the velocity of contraction (v) and the force (F) the heart produces, since the power output (P) of the heart is P = F*v. Two key factors affecting the ensemble force ($F_{ensemble}$) of the heart are the intrinsic force ($F_{intrinsic}$) of each myosin molecule, and the rate of the actin-activated myosin ATPase ($k_{cat} = 1/t_c$, where t_c is the ATPase cycle time). Thus, $F_{ensemble} = F_{intrinsic}(t_s/t_c)N_a$, where t_s is the strongly bound time of a myosin head to actin for one cycle, t_s/t_c is the duty ratio or the fraction of heads bound and producing force at a particular time during contraction, and N_a is the total number myosin heads in the muscle accessible for interacting with actin.

The first measurements with two HCM mutant forms of purified human β-cardiac myosin, R403Q and R453C, appeared to fit this concept. R403Q showed a 25% increase in actin-activated ATPase activity and a 15% increase in velocity (Nag *et al.*, 2015), as measured using the in vitro motility

assay, compared to wild type human β-cardiac myosin, and R453C showed a 50% increase in $F_{intrinsic}$ (Sommese *et al.*, 2013), as measured with a dual beam laser trap. However, as seen in Table 1 (blue columns), filling in the matrix of measurements of ATPase, $F_{intrinsic}$, and velocity for these two mutants as well as others indicated that while one parameter was increased for a particular mutation, other parameters for that mutation were often decreased, making it difficult to see how the ensemble of effects could lead to hypercontractility (Sommese *et al.*, 2013; Nag *et al.*, 2015). Furthermore, in two cases, R663H and G741R, no changes were seen in any of these three parameters compared to wild type human β-cardiac myosin (Kawana *et al.*, 2017; Sarkar *et al.*, 2020).

These results were unexpected and perplexing and one night in late 2014, after reading a book called "The Haunted Mesa," a murder mystery by Louis L'Amour based in the Southwest where mountains with flat top surfaces called mesas dominate the landscape, a dream pointed to myosin having a mesa (see https://www.ibiology.org/cell-biology/muscle-biology/#part-4). The next morning, analysis of the conservation of the residues on that relatively flat mesa surface across cardiac myosin species from mouse to man showed an unusual amount of conservation, suggesting there was something important about this surface (Spudich, 2015). Furthermore, when viewed from the correct angle, the majority of the HCM mutations we were studying at the time lay on the myosin mesa (Figure 1A, B). In addition, most of those mutations were changes from positively-charged arginine residues to non-charged residues (Figure 1A, bold residue numbers).

It was therefore proposed that some sarcomeric protein with a domain that is overall negatively charged could be interacting with the myosin mesa of some of the myosin molecules in the sarcomere and keeping them in an OFF state, unable to interact with actin (Spudich, 2015). Such heads could be being held in reserve and released by appropriate signaling mechanisms when higher power output from the heart was needed. A unifying hypothesis for hypercontractility caused by myosin HCM mutations was proposed that most, if not all, myosin HCM mutations are weakening the protein-protein interactions in this OFF state, increasing the number of heads accessible for interacting with actin (N_a) and thereby causing the hypercontractility seen in HCM patients (Spudich, 2015). It was also proposed that MyBP-C might interact with the mesa and that dysregulation of MyBP-C could also lead to changes in N_a (Spudich, 2015), accounting for why the vast majority of HCM mutations occur in the two sarcomere proteins, β-cardiac myosin and MyBP-C. The status of this unifying hypothesis is evaluated in this editorial.

The mesa surface and its role in the stabilization of the sequestered OFF-state

The unusual aspects of the myosin mesa surface compared to other surfaces on the myosin head domain are illustrated in Figure 1. In these figure panels, all the arginine and histidine residues, both positively charged under physiological conditions, in the entire globular head domain of the myosin molecule are highlighted in blue. The first thing of note is that 6 out of the 7 arginine residues at the mesa surface are residues that cause HCM when mutated to a non-charged residue (Alfares *et al.*, 2015). It will be interesting to see whether the one exception, arginine 434, surfaces as an HCM mutation site in the future. Indeed, there is one report of an HCM patient who was screened for mutations in eight sarcomeric genes and this patient had only an R434T mutation (Wang *et al.*, 2014), but there are no additional reports in ClinVar at this time. The single positively-

charged histidine residue, H251, on the mesa surface also causes HCM when mutated. In addition, the HCM residue R403Q seen on the far right of Figure 1A is readily visible from this view of the myosin head domain. Thus, this is a highly HCM-rich surface of the myosin molecule (Spudich, 2015; Homburger *et al.*, 2016). In contrast, rotating the molecule shown in Figure 1A to view the other side (Figure 1C) reveals a more corrugated surface which has no arginine or histidine residues on its surface.

The proximal tail domain of myosin is involved in a sequestered OFF-state known as the Interacting Heads Motif (IHM)

The coiled-coil tail of human β-cardiac myosin is divided into two domains, subfragment 2 (S2), which follows directly after the subfragment 1 (S1) globular heads, and light meromyosin (LMM), which extends to the C-terminus of the molecule. LMM self assembles and forms the shaft of the muscle thick filament, while S2 is free to move away from the thick filament and bring the myosin heads in contact with the actin filaments. We define the proximal part of S2 (proximal S2) as the first ~15 heptads of the coiled coil.

Another important protein-protein interaction, that of the proximal S2 of the myosin with its own globular S1 domain, derives from the groundbreaking studies by Susan Lowey and Kathy Trybus (Trybus, Huiatt and Lowey, 1982; Trybus and Lowey, 1984; Lowey and Trybus, 1995, 2010; Trybus *et al.*, 1997) and then expanded by the laboratories of Ken Taylor (Wendt *et al.*, 1999, 2001; Liu *et al.*, 2003, 2006; Tama *et al.*, 2005; Rahmani *et al.*, 2021; Chen *et al.*, 2024), Roger Craig (Woodhead *et al.*, 2005; Jung, Komatsu, *et al.*, 2008; Zoghbi *et al.*, 2008; Zhao, Craig and Woodhead, 2009; Yang *et al.*, 2020), Raul Padron (Alamo *et al.*, 2008, 2018; Sulbarán *et al.*, 2015; Dutta *et al.*, 2023), Matthias Gautel (Blankenfeldt *et al.*, 2006), Stefan Raunser (Tamborrini *et al.*, 2023), and others (Offer and Knight, 1996; Burgess *et al.*, 2007; Jung, Burgess, *et al.*, 2008; Jung *et al.*, 2011; Al-Khayat *et al.*, 2013; Scarff *et al.*, 2020; Heissler *et al.*, 2021). Thus, a relevant protein interaction with the myosin mesa could be the proximal tail of the very same myosin molecule causing the two heads of the myosin to fold back onto its own tail in a structural OFF state that has been termed the interacting heads motif (IHM) (Wendt *et al.*, 2001; Woodhead *et al.*, 2005; Burgess *et al.*, 2007; Al-Khayat *et al.*, 2013; Woodhead, Zhao and Craig, 2013; Lee *et al.*, 2018; Craig and Padrón, 2022).

The high-resolution structure of the human β-cardiac myosin IHM state supports the unifying hypothesis

The IHM is said to have a blocked head (its actin binding face is clearly not able to bind to actin) and a free head (the actin binding domain is more accessible) (Figure 2). Margaret Sunita, a postdoctoral fellow in the Spudich/Ruppel laboratory, created homology models of human β-cardiac myosin folded into the IHM state (e.g. MS03 (Nag *et al.*, 2017), https://spudlab.stanford.edu/homology-models), and this model made it immediately apparent that the cluster of positively-charged arginine residues on the myosin mesa that cause HCM when mutated are in the vicinity of a cluster of negatively-charged glutamate and aspartate residues in the proximal tail of the myosin, many of which also cause HCM when mutated (Spudich, 2015; Homburger *et al.*, 2016). Two other homology models of the human β-cardiac myosin IHM, PDB

code 5TBY (Alamo *et al.*, 2017) and PDB code MA1 (Robert-Paganin, Auguin and Houdusse, 2018) similarly predicted that the major molecular consequence of several HCM mutations appeared to be the disruption of IHM interactions stabilizing the sequestered state of myosin. Alamo *et al.* (2017) and Robert-Paganin *et al.* (2018) have discussed in great details the proposed direct and indirect effects of over 100 pathogenic HCM variants on the stability of IHM, and both these models have also been used to predict the effects of several dilated cardiomyopathy (DCM) mutations on the IHM. Overall, the three models have been very useful for many studies, but they are only rough models, and furthermore do not provide the resolution sufficient to say anything about specific sidechain interactions, and in our publications we have emphasized that the actual structure of the human β-cardiac myosin IHM could be quite different from the homology models and was of high priority to obtain.

In 2023, a 3.6 Å resolution structure of the human β-cardiac myosin IHM was solved, which indeed is significantly different in many important ways from any of the earlier homology models, as described (Grinzato *et al.*, 2023). All previous models were wrong in significant ways (as described in the Grinzato *et al.*, 2023 paper). Three high resolution cryo-EM structures of smooth muscle myosin IHM were reported not long before the human β-cardiac myosin IHM structure was determined (Scarff *et al.*, 2020; Yang *et al.*, 2020; Heissler *et al.*, 2021), and it was suggested that homology modeling based on these structures might reveal the effects of HCM mutations on cardiac IHM (Scarff *et al.*, 2020). But comparisons of smooth muscle myosin and cardiac myosin IHM structures revealed major differences between them (Grinzato *et al.*, 2023), establishing that such smooth muscle IHM based analyses would have been wrong too. The high-resolution structure of the isolated human β-cardiac myosin IHM is compatible with the IHM observed in relaxed filaments solved at medium to low-resolution by cryo-EM and cryo-ET published recently (Dutta *et al.*, 2023; Tamborrini *et al.*, 2023). However, the high-resolution structure (PDB 8ACT, (Grinzato *et al.*, 2023)) is the only one to provide atomic details needed to establish which conformation the heads must adopt to form the asymmetric IHM configuration.

The new structure reveals the same clustering of positively-charged arginine residues on the myosin mesa of the blocked head of the IHM near the proximal S2 (Figure 2A, B, C), as observed in the MS03 homology model (Nag *et al.*, 2017), and it is likely that a general charge-charge interaction between this arginine-rich cluster and the negatively-charged nearby region of the proximal S2 (Figure 2, red residues; those shown as spheres being residues that when mutated cause HCM) is helping to stabilize the IHM state. And as was proposed earlier (Spudich, 2015, 2019; Spudich *et al.*, 2016; Alamo *et al.*, 2017; Nag *et al.*, 2017; Robert-Paganin, Auguin and Houdusse, 2018; Trivedi *et al.*, 2018), single residue changes in either of these clusters might result in weakening the IHM state, which results in more myosin heads being put in play for interaction with actin. In the recent paper on the high-resolution structure of the human β-cardiac myosin IHM, it was pointed out that only arginine 453 has specific contacts with the proximal S2 (Grinzato *et al.*, 2023). One important perspective, however, is that the mesa-proximal S2 interaction might not be dominated by specific sidechain interactions, but rather a more diffuse yet overall strong electrostatic interaction formed by a cloud of negative charges on the proximal S2 and a cloud of positive charges on the blocked head. Thus, the proximal S2 domain shown in Figure 2 might not be fixed in position as shown in this static structure but might be able to dynamically access the

broader positively-charged mesa surface. This complementary electrostatic charge surface is likely a prerequisite to form the IHM and to allow a dynamic on/off switch of the heads either packed against the thick filament or available for participating in contraction. In fact, further investigation revealed that the S2 coiled-coil can adopt different positions on the surface of the blocked head when IHM are in solution (Houdusse lab and Spudich lab, unpublished results), in agreement with the role of these complementary long range and dynamic interactions. The same arguments might apply to the head-head interaction site. Interestingly, unlike the earlier MS03 homology model where the head-head interaction site on the free head side involved primarily the converter domain (Nag *et al.*, 2017), the 3.6 Å resolution structure of the human β-cardiac myosin IHM shows that a good portion of the free head mesa domain is involved (Grinzato *et al.*, 2023) (Figure 2D, E). The HCM residues R169G, R453C, H251N, R249Q and R663H are all near this interface. As reported earlier, in the static structure interactions are seen only with R169, R453 and H251 (Grinzato *et al.*, 2023). But again, in the context of the dynamic structure, the overall cluster of positive charge might be playing a role in the formation and stabilization of the IHM.

The correlation of the importance of such dynamic and plastic charge-charge interactions for the tuning of the heads available for heart contraction is that the IHM would be poised to unfold its heads with just a single charge change, such as any of the HCM arginine residues shown in Figure 2, by way of an overall change of the net charge involved in a charge cluster. As discussed below, however, HCM mutations nearly anywhere in the molecule appear to weaken the IHM state. Thus, the very precise structure of the human β-cardiac myosin IHM appears to be required to maintain the normal wild-type level of IHM heads in a population of myosin molecules. If the cloud cluster concept dominated the stability of the IHM state, then one would expect that primarily those HCM residues at protein-protein interaction sites cause an opening of heads, while HCM mutations elsewhere in the molecule might be predominantly causing changes in one of the three fundamental parameters of ATPase, $F_{intrinsic}$, and velocity. As described below, this is not the case.

MyBP-C regulates the stability of the sequestered OFF-state

One sarcomeric protein that could stabilize the heads in an OFF state is myosin binding protein C (MyBP-C). This proposal (Spudich, 2015, 2019; Spudich *et al.*, 2016; Trivedi *et al.*, 2018) made sense given that mutations in the genes giving rise to β-cardiac myosin and MyBP-C account for ~80% of all known HCM mutations. MyBP-C has been shown in multiple studies to inhibit myosin interaction with actin, potentially by sequestering heads away from the thin filament (Gruen and Gautel, 1999; Gruen, Prinz and Gautel, 1999; Ababou, Gautel and Pfuhl, 2007; Oakley *et al.*, 2007; Ababou *et al.*, 2008; Ratti *et al.*, 2011; Pfuhl and Gautel, 2012; Previs *et al.*, 2012; Kampourakis *et al.*, 2014; Mun *et al.*, 2014; Previs, Michalek and Warshaw, 2014; Moss, Fitzsimons and Ralphe, 2015; Inchingolo *et al.*, 2019; Rahmanseresht *et al.*, 2021; Brunello and Fusi, 2024). Indeed, Nag, Trivedi *et al*. (Nag *et al.*, 2017) showed that MyBP-C binds to the single-headed human β-cardiac myosin subfragment 1 (S1), consistent with this idea. Thus, HCM-causing mutations in MyBP-C that lead to haploinsufficiency and decreased levels of MyBP-C in the sarcomere would result in more heads available for interaction with actin, resulting in hypercontractility. Furthermore, like mutations on the myosin mesa, point mutations in MyBP-C that cause HCM may also be weakening the proposed MyBP-C/myosin head interaction. Measurements in muscle fibers from

HCM patients indicate that mutations in *MyBPC3* decrease the level of SRX (super relaxed state), a low energy state of myosin (Hooijman et al, 2011) associated with the IHM structural state. These results support a role of this protein in stabilizing the IHM (McNamara *et al.*, 2017; Toepfer *et al.*, 2019). Nelson *et al.* recently elegantly determined the sub-sarcomeric location of SRX myosin in isolated mouse cardiac myofibrils (Nelson *et al.*, 2023). Determination of the location of individual fluorescent-ATP turnover events using super-resolution microscopy revealed the presence of SRX myosin in a gradient along the thick filament: highest in the C and P zones and lower in the D zone which lacks MyBP-C and lies farthest from the sarcomere center, suggesting that MyBP-C possibly stabilizes SRX myosin. Interestingly, myofibrils from *MYBPC3* null mice displayed roughly 40% reduction in SRX myosin in both C and D zones, suggesting that the effect of MyBP-C on SRX stability somehow extends beyond the C-zone. Similarly, Pilagov *et al.* observed a gradient of SRX myosin heads in skeletal muscle myofibers using a similar experimental approach (Pilagov *et al.*, 2023), supporting a role for MyBP-C in regulating the stability of SRX myosin. HCM mutations in both myosin and MyBP-C can weaken this regulatory interaction, which may alter the stability of SRX myosin. A few HCM mutations in *MYH7* (R403Q, R870H, E924K and E930del) (Sarkar *et al.*, 2020; Singh, McNamara and Sadayappan, 2021) and *MYBPC3* (R502W) (Sen-Martín *et al.*, 2024) have indeed been shown to weaken myosin-MyBP-C interaction.

More biochemical measurements are needed to understand the role of myosin and MyBP-C in regulation of contraction, but structural insights are critical to map the elusive myosin/MyBP-C binding interfaces. The recent cryo-EM and cryo-ET structures of the cardiac filament in relaxed conditions allow one to visualize for the first time the interactions between cardiac IHM and MyBP-C (Dutta *et al.*, 2023; Tamborrini *et al.*, 2023). In these structures, the cardiac filament has a typical three-fold pseudo-symmetry, and the MyBP-C interacts with two of the IHM crowns: the horizontal crown (CrH) and the tilted crown (CrT) (Dutta *et al.*, 2023; Tamborrini *et al.*, 2023) (Figure 3A). Three sites of interaction can be described from these structures. On the CrH, MyBP-C forms two regions of interaction with the free head: the C5 domain interacts with the RLC, and the C8 domain interacts with the U50 subdomain of the myosin head (Figure 3B). The U50 domain of the CrT interacts with the C10 domain of MyBP-C (Figure 3C). These interactions support the hypothesis that the MyBP-C can stabilize the IHM. The mesa is mainly involved in the interfaces between the myosin heads and is found on the other side of the myosin/MyBP-C interfaces. The third crown on the relaxed filament appears disordered (CrD) and is far away from the MyBP-C C5-C10 domains.

The resolution of the current structures of the cardiac filament in relaxed conditions is not sufficient to describe the interactions between the IHMs and the MyBP-C at an atomic level. Further investigations are critically needed to precisely define the role of MyBP-C on the dynamic formation/destabilization of the IHM motifs.

Biochemical assays for measuring the percentage of myosin heads in the IHM state are essential

While structures are critical for understanding mechanisms of protein function, they can only lead to hypotheses, and biochemical assays are essential for examining, in this case, whether myosin HCM mutations liberate heads from an OFF state so there are more myosin heads accessible for

interaction with actin. One biochemical assay that has been used to examine whether HCM mutations liberate myosin heads from an OFF state is the SRX assay already mentioned above, developed by Roger Cooke and his colleagues. These investigators made the important discovery that in relaxed fibers from both skeletal and cardiac muscle there exists a state of myosin that has extremely low basal ATPase activity, meaning the level of myosin ATPase in the absence of actin interaction (Stewart *et al.*, 2010; Cooke, 2011; Hooijman, Stewart and Cooke, 2011; Naber, Cooke and Pate, 2011). The assay they developed involves loading fluorescently labeled ATP (mant-ATP) onto the myosin in permeabilized muscle fibers and measuring the rate of release of fluorescent nucleotide after chasing with excess unlabeled ATP. They called the population of heads having a very low basal ATPase rate the super relaxed state (SRX). The population of heads with normal basal activity is called the disordered state (DRX) and their ATPase activity is quite low compared to the actin-activated ATPase rate, but the SRX rate is an order of magnitude lower than the normal basal rate, thus preserving energy utilization when the muscle is at rest. They estimated that about half of the myosin molecules in the relaxed state of the muscles are in the SRX state. In cardiac muscle, unlike skeletal muscle, these SRX heads remain even after the muscle is activated for contraction (Stewart *et al.*, 2010; Hooijman, Stewart and Cooke, 2011; McNamara *et al.*, 2015). Thus, in cardiac muscle the SRX heads appear to be being held in reserve and are only activated when an increased power output of the heart is needed physiologically, for example by phosphorylation of the myosin RLC by myosin light chain kinase. Rohde *et al.* (Rohde *et al.*, 2018), subsequently showed that the SRX state can be observed using purified bovine cardiac myosin, and Anderson *et al.* (Anderson *et al.*, 2018) showed the same with purified human β-cardiac myosin, which has about 40% of its myosin heads in the SRX state, indicating that this state is linked to a conformation the myosin heads can adopt, rather than their sequestration by interactions with other components of the sarcomere.

This SRX assay has been used to estimate the fraction of heads in a presumed IHM OFF state in tissue samples of HCM patients and in iPSC-derived cardiomyocyte cell lines (Table 2). In 2017, McNamara *et al.* (McNamara *et al.*, 2017) reported for the first time the presence of SRX myosin in human left ventricular (LV) tissue and showed that missense and truncation HCM mutations in *MYBPC3* disrupted SRX myosin using LV tissue samples obtained from HCM patients during myectomy surgery. Similar observations of decreased SRX myosin proportion in human HCM heart fibers with the heterozygous *MYH7* mutation R663H (Anderson *et al.*, 2018) or *MYBPC3* truncations (caused by frame-shift mutations: N981fs, L1014fs and K1209fs) (Toepfer *et al.*, 2019) have been made by other investigators. More recently, to better understand the early mechanisms of HCM disease manifestation due to mutations in *MYH7*, investigators from several laboratories have used cardiomyocytes derived from human induced pluripotent stem cells (hiPSC-CMs) CRISPR-edited to harbor a pathogenic HCM mutation in one of the *MYH7* alleles as model systems (Toepfer *et al.*, 2020; Vander Roest *et al.*, 2021; Lee *et al.*, 2024). HCM mutations have been reported to evoke several key features of HCM pathophysiology including increased contractile function, altered cell size and myofibril organization, and altered cellular metabolism in these hiPSC-CM model systems. Three HCM mutations in *MYH7* studied using the iPSC-derived cardiomyocyte cell lines – R403Q, V606M and R719W – were found to significantly decrease the proportion of myosins in the SRX state (Toepfer *et al.*, 2020). Overall, in all cases examined, a decrease in SRX was observed, consistent with the hypothesis that HCM mutations

cause a decrease in the number of heads held in a sequestered OFF-state, and this was true for HCM mutations in both MYH7 and *MYBPC3*, in keeping with the general unifying hypothesis.

Importantly, a similar level of SRX (40-50%) as seen in muscle fibers is also observed in purified human β-cardiac myosin preparations fully reconstituted with human β-cardiac myosin light chains (Adhikari *et al.*, 2019; Sarkar *et al.*, 2020; Vander Roest *et al.*, 2021; Morck *et al.*, 2022; Lee *et al.*, 2024; Nandwani *et al.*, 2024) (Table 1). Notably, as for the tissue samples of HCM patients and iPSC-derived cardiomyocytes, an HCM-induced increase in SRX has not been seen in these purified protein studies. All results show a decrease in SRX, consistent with the assumed increase in the number of heads accessible for interaction with actin caused by HCM mutations. Interestingly, the opposite was recently reported for two dilated cardiomyopathy (DCM) associated mutations, E525K in the heavy chain (Rasicci *et al.*, 2022; Duno-Miranda *et al.*, 2024) and D94A in the RLC (Yuan *et al.*, 2022), both of which show an increase in SRX, and the assumed decrease in the number of myosin heads available for force production is proposed to be the primary mechanism of hypocontractility associated with these mutations. A logical assumption has been that the biochemical SRX state can be equated with the structural IHM state. However, the situation is more complicated than this, as described below, and caution needs to be exercised in using this indirect assay.

A direct biochemical assay for measuring whether an HCM mutation is causing the release of more myosin heads for interaction with actin involves comparing the actin-activated ATPase activity of two different 2-headed human β-cardiac myosin constructs - a short-tail construct (2-heptad repeat, or more recently 8-heptad), which cannot form the IHM state, with the actin-activated ATPase activity of a long-tail construct (25-heptad repeat, or more recently a 15-heptad proved to be sufficient), which can form the IHM state (Nag *et al.*, 2017; Anderson *et al.*, 2018; Grinzato *et al.*, 2023; Nandwani *et al.*, 2024) (Figure 4A). The actin-activated ATPase activity of a long-tail construct is typically 40-50% lower than its corresponding short-tailed construct (Figure 4B), presumably because the long-tail construct can form the IHM OFF state. Of more than 100 measurements over several years assessing the ratio of actin-activated ATPase for the long-tail myosin wild type construct and the short-tail myosin wild type construct, the value has consistently been between 0.5 and 0.6, with the average value being 0.57. This is presumably due to 43% of the population of wild type human β-cardiac myosin existing in an IHM state. If an HCM mutation destabilizes the putative IHM state in these biochemical measurements, then the long-tail constructs will approach the ATPase values of the short-tail constructs. We call this the long-tail/short-tail ATPase ratio (LSAR) assay.

The LSAR assay can be used to examine effects of physiologically-relevant biochemical changes to wild type myosin as well as of HCM mutations

Nag *et al*. (Nag *et al.*, 2017) used the LSAR assay to examine the effects of RLC phosphorylation on the number of OFF-state heads in a myosin population. In their experiments, a short-tail myosin construct showed the same level of actin-activated ATPase whether the RLC is phosphorylated. However, a long-tail construct in the absence of phosphorylation showed a reduction in actin-activated ATPase presumably because a significant percentage of the myosin heads in the non-phosphorylated state are in an IHM state, and phosphorylation of the RLC of the long-tail myosin

largely eliminates the OFF-state population (Figure 4C). This directly demonstrates biochemically what is probably the physiological role of RLC phosphorylation in cardiac muscle, as described for multiple myosin types previously (Craig, Padrón and Kendrick-Jones, 1987; Padrón *et al.*, 1991; Cremo, Sellers and Facemyer, 1995; Levine *et al.*, 1996; Trybus *et al.*, 1997; Wendt *et al.*, 1999; Alamo *et al.*, 2008, 2015; Lowey and Trybus, 2010; Scruggs and Solaro, 2011; Toepfer *et al.*, 2013; Espinoza-Fonseca *et al.*, 2015; Kampourakis and Irving, 2015; Vandenboom, 2016; Trivedi *et al.*, 2018).

When using the LSAR assay to measure whether HCM mutations cause an increase in the LSAR, which indicates the opening of heads from a sequestered state, all experiments have used constructs with the RLC in its non-phosphorylated state. Furthermore, for every mutation, both the mutant short-tail version and the mutant long-tail version were made and the actin-activated ATPase of the two were compared. This comparison is essential since some HCM mutations result in a change in the fundamental actin-activated ATPase rate parameter of the short tail version (Table 1, first blue column), also seen in single-headed S1 experiments (Nag *et al.*, 2015; Adhikari *et al.*, 2016, 2019; Vera *et al.*, 2019; Morck *et al.*, 2022; Nandwani *et al.*, 2024).

Twenty HCM mutations have now been analyzed using both the LSAR and SRX assays (Table 1), and there are several important conclusions. First and foremost, 19 of the 20 total show an increase in the number of myosin heads in the ON state using the LSAR assay, presumably by weakening the IHM configuration. The single mutation that did not show an increase in heads in an ON state using the LSAR assay, I457T, demonstrated a large 75% increase in actin-activated ATPase and a 240% increase in velocity (Table 1, blue columns) (Adhikari *et al.*, 2019). These values significantly exceed the changes in these fundamental parameters observed for any of the other mutations, and presumably account for the hypercontractility caused by the I457T mutation. The bottom-line, however, is that it is likely that most HCM mutations in myosin cause an increase in the number of heads available for interaction with actin (N_a), and the unifying hypothesis proposed in 2015 (Spudich, 2015) is in good stead.

From a structural standpoint, 6 out of the 20 HCM residues that have been analyzed using the LSAR assay are in the vicinity of protein-protein interfaces of the IHM state (Figure 5), R249Q on the blocked head at the head-proximal S2 interaction site (blue residue), D382Y and R403Q on the blocked head at the head-head interaction site (yellow residues), R719W on the free head at the head-head interaction site (orange residue), and H251N and R663H, which are near both the blocked head-proximal S2 interaction site and the head-head interaction site. Not all of these 6 are necessarily playing a role at the relevant interfaces (Grinzato *et al.*, 2023), but the remaining 14 analyzed HCM residues (Figure 5, magenta residues) are clearly not at the protein-protein interaction sites. Yet, 13 of them cause an opening of the heads from the IHM OFF state (Table 1). This is highly significant because those mutations must be altering the detailed atomic-resolution features of the molecule rather than causing a change in a surface charge cluster described above. This is why a high-resolution structure of the human β-cardiac myosin IHM was essential, since it allows one to study the interfaces stabilizing the motif at an atomic level and to describe the precise effect of each HCM-causing mutation.

The fact that many of the HCM mutations that cause an increase in N_a do not lie at obvious interfaces between the two myosin heads or the interface between the blocked head and the proximal S2 (see Table 1 and Figure 5) emphasizes that one cannot predict from the structure alone whether a particular mutation is likely to increase N_a. This is because myosin is a highly dynamic and allosteric protein and mutations anywhere can propagate changes to the other parts of the protein and influence the stability of the IHM state. Thus, it is essential to carry out the LSAR biochemical assay to determine whether the effects of a particular mutation increase N_a. This cannot be determined by analysis of the IHM structure alone.

The second major observation from the data in Table 1 is that while 13 of these HCM mutations also show a decrease in the number of SRX heads, 7 of them do not. This emphasizes that while the SRX assay appears to be reasonably good at predicting an opening up of myosin heads, it must not be used as a definitive assay to establish whether molecules in the IHM OFF state are being liberated for interaction with actin because of the mutation. This caution goes along with the results of Anderson, Trivedi *et al*. (Anderson *et al.*, 2018) which showed that both a short tail version of human β-cardiac HMM and single-headed S1 show a significant amount of SRX activity. This was also observed for bovine cardiac S1 by Rohde, *et al*. (Rohde *et al.*, 2018). These results establish that an IHM state is not needed for cardiac myosin to be in an SRX state, and IHM and SRX must not be equated, as also indicated by results from other groups (Chu, Muretta and Thomas, 2021; Craig and Padrón, 2022; Walklate *et al.*, 2022; Ma *et al.*, 2023; Jani *et al.*, 2024). Recently, some have even questioned whether distinct SRX and DRX populations can be observed using purified proteins in the mant-ATP single turnover assay (Mohran *et al.*, 2024), though the discrepancies between their findings and those of other laboratories (Anderson *et al.*, 2018; Rohde *et al.*, 2018; Adhikari *et al.*, 2019; Sarkar *et al.*, 2020; Vander Roest *et al.*, 2021; Rasicci *et al.*, 2022; Lee *et al.*, 2024; Nandwani *et al.*, 2024) will take time to sort out. In any case, the only reliable and direct biochemical assay for measuring whether an HCM mutation is causing more heads to become available for interaction with actin is the LSAR assay.

Two small molecule inhibitors of human β-cardic myosin have been developed to reverse the effects of HCM-induced hypercontractility

While conventional therapies for HCM are aimed toward controlling the hyperactive physiology caused by the disease, until recently none have been directed toward inhibiting the human β-cardiac myosin directly. Over the last decade, however, two small molecule inhibitors that bind directly to the β-cardiac myosin head domain and inhibit its actin-activated ATPase activity have been described, mavacamten (Green *et al.*, 2016) and aficamten (Chuang *et al.*, 2021). Both molecules were developed with the concept that if one could reduce the hypercontractility to normal this could reduce the negative effects of the hypercontractile state and possibly prevent or even reduce existing hypertrophy of the heart (Green *et al.*, 2016; Heitner *et al.*, 2019; Spudich, 2019; Hegde *et al.*, 2021; Saberi *et al.*, 2021; Day, Tardiff and Ostap, 2022; Kawana, Spudich and Ruppel, 2022; Lehman, Crocini and Leinwand, 2022; Maron *et al.*, 2023).

Mavacamten reverses the primary action of HCM mutations by putting myosin heads back into a 2-headed-compact sequestered OFF state, as possibly suggested by EM (Anderson *et al.*, 2018) and small angle X-ray scattering studies (Gollapudi *et al.*, 2021). It is not clear whether

mavacamten binding puts myosin heads back into an IHM state or into some other 2-headed-compact state (Figure 6) (Chu, Muretta and Thomas, 2021; Gollapudi *et al.*, 2021; Nag *et al.*, 2023). In the cryo-EM and cryo-ET studies where the thick filament is relaxed by mavacamten (Dutta *et al.*, 2023; Tamborrini *et al.*, 2023), the structure of the IHM seems similar to that of apo classical IHMs (Grinzato *et al.*, 2023). Thus, it will be essential to determine the high-resolution structure of the mavacamten-bound two-headed myosin to depict how the drug influences the conformation and dynamics of the IHM. Interestingly, molecular dynamics based on the crystal structure of cardiac myosin complexed to mavacamten demonstrated that mavacamten explores different positions in its allosteric binding pocket, which influences the dynamics of the lever arm as well as the allostery within the myosin head (Auguin *et al.*, 2023). It is thus likely that the conformational space explored by the IHM in presence of mavacamten differs. In addition, mavacamten also acts by inhibiting the ability of a free head to produce force on F-actin (Auguin *et al.*, 2023). In sum, mavacamten fundamentally reverses the effects of the HCM mutations in that the mutations are largely liberating heads from a sequestered OFF state and mavacamten is returning active heads back to a sequestered OFF state or slows their ability to bind and produce force on F-actin.

Conclusion

The results of the last nine years have led to considerable evidence in support of the unifying hypothesis that the key mechanism of HCM-induced hypercontractility is the release of myosin heads from a sequestered OFF state, putting more heads in play for interaction with actin. The OFF state has now been depicted at high resolution revealing the interactions that stabilize the asymmetric IHM state (Grinzato *et al.*, 2023), which is further sequestered on the thick filament by interactions with MyBP-C (Dutta *et al.*, 2023; Tamborrini *et al.*, 2023). We suggest that this unifying hypothesis not only pertains to HCM mutations in myosin but to HCM mutations in other sarcomeric proteins as well. As discussed above, the majority of HCM-causing mutations in *MYBPC3* lead to haploinsufficiency and therefore less MyBP-C to sequester myosin heads.

While the LSAR assay is the best assay for measuring changes in N_a for myosin HCM mutations, so far it has been applied only in the context of purified human β-cardiac myosin alone. Many of the myosin HCM mutations might require additional components for the effects on N_a to be seen. In the context of the thick filament, the heads of one myosin molecule interact with the heads of an adjacent molecule, and some HCM mutations in the myosin head may be affecting this stabilizing interaction, causing a weakening of the OFF-state (Grinzato *et al.*, 2023; Dutta *et al.*, 2024). In particular, HCM mutations in the myosin rod might involve residues that are involved in or interacting with the light-meromyosin (LMM) core of the thick filament or interacting with other protein components of the thick filament. In the proximal S2, for example, there is a hot spot for HCM mutations in the first 4.5 heptads of the rod, many of which are changes from positively charged arginine and lysine residues to negatively charged or uncharged residues (Figure 7). This region of the coiled-coil is not obviously involved in stabilizing the IHM configuration in isolation of the thick filament according to the recent high-resolution WT structure (Grinzato *et al.*, 2023), and it is also ~4-5 nm away from the LMM core or other proteins currently modeled from the thick filament maps in the relaxed state (Dutta *et al.*, 2023; Tamborrini *et al.*, 2023). While it cannot be

excluded that this cluster of positive residues might interact by a weak charge-charge interaction with a net negative region of another protein of the thick filament to stabilize the OFF-state, it is likely that the mutations affect the dynamics/stability of the coiled-coil itself, thus leading to destabilization of the OFF-state configuration. Indeed, these residues are involved in van der Waals and electrostatic interactions between the two strands of the proximal S2 according to our high-resolution structure (Grinzato *et al.*, 2023). These possibilities can now be explored by characterization of mutant recombinant cardiac myosin with the LSAR, biophysical and structural assays. Further elegant cryo-electron microscopy and tomography maps of the mutants of cardiac thick filament studied up to ~6 Å and ~18 Å resolution, respectively, as recently described for WT cardiac samples (Dutta *et al.*, 2023; Tamborrini *et al.*, 2023) should also be performed to get a holistic description of how distinct mutations affect the number of heads in the OFF-state on the thick filament in relaxed conditions. By combining our 3.6 Å IHM structure with these cardiac thick filament reconstructions, it is now possible to analyze how these and other myosin HCM mutations might be affecting the IHM OFF-state in the context of the thick filament.

Regarding the issue of using SRX as an assay for measuring an increase in N_a, the data in Table 1 emphasizes that caution should be used in interpreting SRX data. On the positive side, an SRX increase has not been seen in any of the HCM mutant studies, which would have suggested an increase of heads in an OFF-state (Rasicci *et al.*, 2022; Yuan *et al.*, 2022), and the decreases in SRX found have always been confirmed with the LSAR assay. But there are 7 cases where a clear increase in N_a is seen by the LSAR assay that is not reflected in the SRX assay. Thus, the direct LSAR assay is the preferred approach but has the limitation that it can only be applied to examination of purified proteins.

Finally, along with a better understanding of the mechanistic basis of HCM-induced hypercontractility has come new therapies for HCM that target the human β-cardiac myosin directly with small molecules that remove myosin heads from accessibility to actin interaction, thus normalizing the contractility of the heart.

Future directions

Regulation of the autoinhibited OFF state of myosin now appears to be a key determinant of cardiac contractility and energy utilization. Pathogenic mutation-associated alterations in myosin's conformational dynamics are beginning to be associated with myopathies other than HCM including DCM and atrial cardiomyopathy (mutations in *MYH6*; Kawana *et al.*, unpublished results). In the past few years, alterations in the sequestered OFF state stability by DCM-causing mutations has been observed for two mutations in myosin heavy (E525K) and light chains (D94A in RLC); both mutations were found to result in stabilization of the SRX state (Rasicci *et al.*, 2022; Yuan *et al.*, 2022; Duno-Miranda *et al.*, 2024), which is predicted to lead to hypocontractility due to reduced number of myosin heads available for force production. FRET-based assays, negative-staining EM analysis and comparison of the actin-activated ATPase rates and in-vitro velocities for long and short-tailed constructs of E525K indicate that the hypocontractility associated with this DCM mutant can be attributed primarily to increased sequestration of myosin heads in the IHM/SRX state (Rasicci *et al.*, 2022; Duno-Miranda *et al.*, 2024). DCM, however, is more heterogenous than HCM and may lack a unifying mechanism of disease manifestation, as indicated

by results from other studies where pathogenic mutations including the novel severe early-onset DCM mutation Q222H (Kawana *et al.*, 2023) and R369Q (Nandwani *et al.*, unpublished results) were investigated and were found to not affect the SRX-DRX equilibrium.

Recent studies have implicated the destabilization of the OFF state of *MYH7* in the pathogenesis of skeletal myopathy as well. Using muscle biopsy specimens obtained from patients, molecular analysis of 10 distinct *MYH7* mutations in the light-meromyosin (LMM) core of the thick filament, which result in skeletal muscle diseases rather than cardiomyopathies, found a significant decrease in the proportion of SRX myosin (Carrington *et al.*, 2023; Buvoli *et al.*, 2024). It remains to be seen how altered SRX-DRX equilibrium contributes to the pathophysiology of skeletal muscle myopathies.

Acknowledgements

We acknowledge funding by NIH R01 GM33289 (J.A.S.), ANR-21-CE11-0022-01 (A.H.), NIH RM1 GM131981-01 (J.A.S. and A.H.), and AHA postdoctoral award 22POST908934 (N.N.).

Competing Interest Statement

J.A.S. is cofounder and on the Scientific Advisory Board of Cytokinetics, Inc., a company developing small molecule therapeutics for treatment of hypertrophic cardiomyopathy. J.A.S. is cofounder and Executive Chairman, and K.M.R. is cofounder & Research and Clinical Advisor, of Kainomyx, Inc., a company developing small molecule therapeutics targeting myosins in parasites. A.H. receives research funding from Cytokinetics and consults for Kainomyx.

Legends

Figure 1. The myosin mesa and hypertrophic cardiomyopathy mutations. (A) The blocked head of the high-resolution human β-cardiac myosin OFF state (PDB 8ACT) showing a top view of the flat myosin mesa (red dashed oval), with the 6 arginine-based HCM residues and single non-HCM-producing arginine, arginine 434 shown in dark blue. The single histidine-based HCM residue (light blue), H251, is also shown. The position of the myosin converter domain is illustrated by the purple oval. The myosin heavy chain is in light grey, the essential light chain (ELC) in light brown, and the regulatory light chain (RLC) in light green. **(B)** The molecule shown in A rotated ~90° to reveal the flatness of the mesa (red dashed line). **(C)** The opposite face of the molecule shown in A. **(D)** The molecule shown in B but with the positions of all the HCM mutations from Table 1 shown. Non-charged residues are shown as magenta spheres.

Figure 2. The 3.6 Å-resolution human β-cardiac myosin IHM structure (PDB 8ACT) with mesa residues at protein-protein interfaces. (A) Pymol cartoon configuration with the 6 arginine-based mesa HCM residues (R169G; R249Q; R442C; R453C; R652G; R663H) shown in dark blue Pymol sphere configuration and the single histidine-based HCM residue (H251N) shown in light blue (all on the blocked head only). The glutamate and aspartate residues in the proximal

S2 near the mesa are colored red, with the four HCM residues (E875del; E894G; E903Q/K; D906G) shown as spheres. The blocked head myosin heavy chain is in light grey, its essential light chain (ELC) in light brown, and its regulatory light chain (RLC) in light green. The free head myosin heavy chain is in dark grey, its ELC in dark brown, and its RLC in dark green. The coiled-coil proximal S2 tail domain is shown in light and dark cyan. **(B)** The same configuration as in panel A, but shown as spheres. The dashed red oval outlines the mesa. **(C)** Blowup of the blocked head mesa region of panel A. **(D)** The molecule in B rotated ~180°. The free head mesa is indicated by the dashed line and the mesa arginine and histidine residues are shown in blue sphere configuration. The free head converter domain is shown in magenta. **(E)** Blowup of the head-head interaction site shown in panel D.

Figure 3. MyBP-C interacts with two IHM motifs in the relaxed cardiac filament. (A) View of the horizontal (CrH) and the tilted crown (CrT) from the structure of the cardiac filament in relaxed conditions ((Dutta *et al.*, 2023), PDB code 8G4L). These two IHM motifs interact with the MyBP-C (in orange). **(B)** Zoom on the CrH, showing the interactions of the free head with the C5 and C8 domains of the MyBP-C. **(C)** Zoom on the CrT, showing the interactions of the free head U50 subdomain with the C10 domain of the MyBP-C.

Figure 4. The long-tail/short-tail ATPase ratio (LSAR) assay. (A) Left, Pymol depiction of a 2-headed human β-cardiac myosin construct with a 2-heptad repeat of its proximal S2 stabilized by a GCN4 insert (blue), with a GFP (green) added to its C-terminus (short-tail construct). Right, Pymol depiction of a two-headed human β-cardiac myosin construct with a 25-heptad repeat of its S2 stabilized by a GCN4 insert, with a GFP added at its C-terminus (long-tail construct). **(B)** Actin-activated ATPase of a wild type short-tail construct (dark blue) compared to a wild type long-tail construct (light blue). Data from (Adhikari *et al.*, 2019). **(C)** Actin-activated ATPase of a wild type short-tail construct without (circles, dark blue) and with (squares, dark blue) RLC phosphorylation compared to a wild type long-tail construct, without (circles, light blue) and with (squares, light blue) RLC phosphorylation. Data from (Nag *et al*, 2017).

Figure 5. Mutations in the early region of the proximal S2. (A) The 3.6 Å-resolution human β-cardiac myosin IHM structure (PDB 8ACT) with HCM mutations affecting charged residues in the first 4.5 heptads of the proximal S2 shown as spheres. **(B)** Image in A rotated ~90°. The mutations are K847E; E848G; R858C,P,S; K865E; R869H; R870H.

Figure 6. Schematic view of the actin-activated myosin ATPase cycle (left) and various forms of OFF states (right). The formation of the OFF-states removes myosin heads from the cycle. The red star indicates mavacamten binding.

Figure 7. Mutations in the early region of proximal S2. (A) The 3.6 Å-resolution human β-cardiac myosin IHM structure (PDB 8ACT) with HCM mutations affecting charged residues in the first 4.5 heptads of the proximal S2 shown as spheres. **(B)** Image in A rotated ~90°. The mutations are K847E; E848G; R858C, P, S; K865E; R869H; R870H.

Table 1. Summary of data available for 22 HCM mutant forms of human β-cardiac myosin. Table showing data collected on important parameters of myosin function and regulation. The three blue columns are measurements of three fundamental parameters that determine power

output from the muscle, where green values contribute to hypercontractility, red values contribute to hypocontractility, and black zeros indicate no change. The white column shows the percent decrease in SRX, setting the baseline for wild type myosin at 55%. Thus, the % decrease SRX = (55-x)/55, where x = the measured SRX level for a particular HCM mutant myosin. The green values are generally assumed to indicate more myosin heads in play leading to hypercontractility, and black zeros indicate no change. The pink column shows the percentage increase in the additional number of myosin heads made accessible for interaction with actin (additional N_a), setting the baseline of 0.57 as 0% additional heads released. The numbers derive from the formula percent additional N_a increase = (x-0.57)/0.43, where x = the measured long-tail short-tail ATPase Ratio (LSAR) for a particular HCM mutant myosin and 0.57 is the average LSAR value for wild type myosin. Thus, if the mutant protein gives the same LSAR value as the wild-type protein of 0.57, then 0% of the myosin heads are released by the mutation. If the mutant protein gives an LSAR value of 1.0, then 100% of the myosin heads are released by the mutation. The 6 residues that lie at the protein-protein interfaces of the IHM OFF-state described later in the text are indicated by symbols.

Table 2. SRX measurements from tissue samples of HCM patients and in iPSC-derived cardiomyocyte cell lines. Table showing percent decrease in SRX estimated from previous studies from mant-ATP experiments from human HCM patient myocardial samples or iPSC-CMs carrying either *MYH7* or *MYBPC3* mutations. % decrease SRX = (WT-x)/WT, where x = the measured SRX level for a particular HCM mutant and wild-type (WT) control data from the same study was used as reference. The green values are generally assumed to indicate more myosin heads in play leading to hypercontractility. (*estimated from Fig. 2F in (Toepfer *et al.*, 2020), #estimated from Fig. 3F in (Toepfer *et al.*, 2019)).

References

1. Ababou, A. *et al.* (2008) 'Myosin Binding Protein C Positioned to Play a Key Role in Regulation of Muscle Contraction: Structure and Interactions of Domain C1', *Journal of Molecular Biology*, 384(3), pp. 615–630.
2. Ababou, A., Gautel, M. and Pfuhl, M. (2007) 'Dissecting the N-terminal Myosin Binding Site of Human Cardiac Myosin-binding Protein C', *Journal of Biological Chemistry*, 282(12), pp. 9204–9215.
3. Adhikari, A.S. *et al.* (2016) 'Early-Onset Hypertrophic Cardiomyopathy Mutations Significantly Increase the Velocity, Force, and Actin-Activated ATPase Activity of Human β-Cardiac Myosin', *Cell Reports*, 17(11), pp. 2857–2864.
4. Adhikari, A.S. *et al.* (2019) 'β-Cardiac myosin hypertrophic cardiomyopathy mutations release sequestered heads and increase enzymatic activity', *Nature Communications*, 10(1), p. 2685.
5. Alamo, L. *et al.* (2008) 'Three-Dimensional Reconstruction of Tarantula Myosin Filaments Suggests How Phosphorylation May Regulate Myosin Activity', *Journal of Molecular Biology*, 384(4), pp. 780–797.

6. Alamo, L. *et al.* (2015) 'Tarantula myosin free head regulatory light chain phosphorylation stiffens N-terminal extension, releasing it and blocking its docking back', *Molecular BioSystems*, 11(8), pp. 2180–2189.
7. Alamo, L. *et al.* (2017) 'Effects of myosin variants on interacting-heads motif explain distinct hypertrophic and dilated cardiomyopathy phenotypes', *elife*, 6, p. e24634.
8. Alamo, L. *et al.* (2018) 'Lessons from a tarantula: new insights into myosin interacting-heads motif evolution and its implications on disease', *Biophysical Reviews*. Springer Verlag, pp. 1465–1477.
9. Alfares, A.A. *et al.* (2015) 'Results of clinical genetic testing of 2,912 probands with hypertrophic cardiomyopathy: expanded panels offer limited additional sensitivity', *Genetics in Medicine*, 17(11), pp. 880–888.
10. Al-Khayat, H.A. *et al.* (2013) 'Atomic model of the human cardiac muscle myosin filament.', *Proceedings of the National Academy of Sciences of the United States of America*, 110(1), pp. 318–323.
11. Anderson, R.L. *et al.* (2018) 'Deciphering the super relaxed state of human beta-cardiac myosin and the mode of action of mavacamten from myosin molecules to muscle fibers.', *Proceedings of the National Academy of Sciences of the United States of America*, 115(35), pp. E8143–E8152.
12. Auguin, D. *et al.* (2023) 'Omecamtiv mecarbil and Mavacamten target the same myosin pocket despite antagonistic effects in heart contraction', *bioRxiv*, p. 2023.11.15.567213.
13. Blankenfeldt, W. *et al.* (2006) 'Crystal structures of human cardiac β-myosin II S2-Δ provide insight into the functional role of the S2 subfragment', *Proceedings of the National Academy of Sciences*, 103(47), pp. 17713–17717.
14. Brunello, E. and Fusi, L. (2024) 'Regulating Striated Muscle Contraction: Through Thick and Thin', *Annual Review of Physiology*, 86(1), pp. 255-275.
15. Burgess, S.A. *et al.* (2007) 'Structures of Smooth Muscle Myosin and Heavy Meromyosin in the Folded, Shutdown State', *Journal of Molecular Biology*, 372(5), pp. 1165–1178.
16. Buvoli, M. *et al.* (2024) 'A Laing distal myopathy–associated proline substitution in the β-myosin rod perturbs myosin cross-bridging activity', *Journal of Clinical Investigation*, 134(9), p. e172599.
17. Captur, G. *et al.* (2014) 'Prediction of Sarcomere Mutations in Subclinical Hypertrophic Cardiomyopathy', *Circulation: Cardiovascular Imaging*, 7(6), pp. 863–871.
18. Carrington, G. *et al.* (2023) 'Human skeletal myopathy myosin mutations disrupt myosin head sequestration', *JCI Insight*, 8(21), p. e172322.
19. Chen, L. *et al.* (2024) 'Structure of mavacamten-free human cardiac thick filaments within the sarcomere by cryoelectron tomography', *Proceedings of the National Academy of Sciences*, 121(9), p.e. 2311883121.
20. Chu, S., Muretta, J.M. and Thomas, D.D. (2021) 'Direct detection of the myosin super-relaxed state and interacting-heads motif in solution.', *The Journal of biological chemistry*, 297(4), p. 101157.
21. Chuang, C. *et al.* (2021) 'Discovery of Aficamten (CK-274), a Next-Generation Cardiac Myosin Inhibitor for the Treatment of Hypertrophic Cardiomyopathy', *Journal of Medicinal Chemistry*, 64(19), pp. 14142–14152.

22. Cooke, R. (2011) 'The role of the myosin ATPase activity in adaptive thermogenesis by skeletal muscle.', *Biophysical reviews*, 3(1), pp. 33–45.
23. Craig, R. and Padrón, R. (2022) 'Structural basis of the super-and hyper-relaxed states of myosin II', *Journal of General Physiology*, 154(1), pp. 1–14.
24. Craig, R., Padrón, R. and Kendrick-Jones, J. (1987) 'Structural changes accompanying phosphorylation of tarantula muscle myosin filaments.', *The Journal of cell biology*, 105(3), pp. 1319–1327.
25. Cremo, C.R., Sellers, J.R. and Facemyer, K.C. (1995) 'Two Heads Are Required for Phosphorylation-dependent Regulation of Smooth Muscle Myosin', *Journal of Biological Chemistry*, 270(5), pp. 2171–2175.
26. Day, S.M., Tardiff, J.C. and Ostap, E.M. (2022) 'Myosin modulators: emerging approaches for the treatment of cardiomyopathies and heart failure', *Journal of Clinical Investigation*, 132(5), p. e148557.
27. Deacon, J.C. *et al.* (2012) 'Identification of functional differences between recombinant human α and β cardiac myosin motors.', *Cellular and molecular life sciences : CMLS*, 69(13), pp. 2261–77.
28. van Dijk, S.J. *et al.* (2009) 'Cardiac myosin-binding protein C mutations and hypertrophic cardiomyopathy: haploinsufficiency, deranged phosphorylation, and cardiomyocyte dysfunction.', *Circulation*, 119(11), pp. 1473–83.
29. Duno-Miranda, S. *et al.* (2024) 'Tail length and E525K dilated cardiomyopathy mutant alter human β-cardiac myosin super-relaxed state', *Journal of General Physiology*, 156(6), p. e202313522.
30. Dutta, D. *et al.* (2023) 'Cryo-EM structure of the human cardiac myosin filament', *Nature*, 623(7988), pp. 853–862.
31. Dutta, D. *et al.* (2024) 'Pathogenic cardiac thick filament variants: A structural perspective', *Biophysical Journal*, 123(3), p. 403a.
32. Espinoza-Fonseca, L.M. *et al.* (2015) 'Sequential myosin phosphorylation activates tarantula thick filament via a disorder–order transition', *Molecular BioSystems*, 11(8), pp. 2167–2179.
33. Gollapudi, S.K. *et al.* (2021) 'Two Classes of Myosin Inhibitors, Para-nitroblebbistatin and Mavacamten, Stabilize β-Cardiac Myosin in Different Structural and Functional States', *Journal of Molecular Biology*, 433(23), p. 167295.
34. Green, E.M. *et al.* (2016) 'A small-molecule inhibitor of sarcomere contractility suppresses hypertrophic cardiomyopathy in mice', *Science*, 351(6273), pp. 617–621.
35. Grinzato, A. *et al.* (2023) 'Cryo-EM structure of the folded-back state of human β-cardiac myosin', *Nature Communications*, 14(1), p. 3166.
36. Gruen, M. and Gautel, M. (1999) 'Mutations in beta-myosin S2 that cause familial hypertrophic cardiomyopathy (FHC) abolish the interaction with the regulatory domain of myosin-binding protein-C.', *Journal of molecular biology*, 286(3), pp. 933–949.
37. Gruen, M., Prinz, H. and Gautel, M. (1999) 'cAPK-phosphorylation controls the interaction of the regulatory domain of cardiac myosin binding protein C with myosin-S2 in an on-off fashion', *FEBS Letters*, 453(3), pp. 254–259.

38. Haland, T.F. *et al.* (2016) 'Strain echocardiography is related to fibrosis and ventricular arrhythmias in hypertrophic cardiomyopathy', *European Heart Journal – Cardiovascular Imaging*, 17(6), pp. 613–621.
39. Harris, S.P., Lyons, R.G. and Bezold, K.L. (2011) 'In the thick of it: HCM-causing mutations in myosin binding proteins of the thick filament.', *Circulation research*, 108(6), pp. 751–764.
40. Hegde, S.M. *et al.* (2021) 'Effect of Mavacamten on Echocardiographic Features in Symptomatic Patients With Obstructive Hypertrophic Cardiomyopathy', *Journal of the American College of Cardiology*, 78(25), pp. 2518–2532.
41. Heissler, S.M. *et al.* (2021) 'Cryo-EM structure of the autoinhibited state of myosin-2', *Science Advances*, 7(52), p. eabk3273.
42. Heitner, S.B. *et al.* (2019) 'Mavacamten Treatment for Obstructive Hypertrophic Cardiomyopathy', *Annals of Internal Medicine*, 170(11), pp. 741-748.
43. Ho, C.Y. *et al.* (2002) 'Assessment of Diastolic Function With Doppler Tissue Imaging to Predict Genotype in Preclinical Hypertrophic Cardiomyopathy', *Circulation*, 105(25), pp. 2992–2997.
44. Ho, C.Y. *et al.* (2009) 'Echocardiographic Strain Imaging to Assess Early and Late Consequences of Sarcomere Mutations in Hypertrophic Cardiomyopathy', *Circulation: Cardiovascular Genetics*, 2(4), pp. 314–321.
45. Homburger, J.R. *et al.* (2016) 'Multidimensional structure-function relationships in human β-cardiac myosin from population-scale genetic variation', *Proceedings of the National Academy of Sciences*, 113(24), pp. 6701–6706.
46. Hooijman, P., Stewart, M.A. and Cooke, R. (2011) 'A new state of cardiac myosin with very slow ATP turnover: A potential cardioprotective mechanism in the heart', *Biophysical Journal*, 100(8), pp. 1969–1976.
47. Inchingolo, A. V. *et al.* (2019) 'Revealing the mechanism of how cardiac myosin-binding protein C N-terminal fragments sensitize thin filaments for myosin binding', *Proceedings of the National Academy of Sciences of the United States of America*, 116(14), pp. 6828–6835.
48. Jani, V.P. *et al.* (2024) 'The structural OFF and ON states of myosin can be decoupled from the biochemical super- and disordered-relaxed states.', *PNAS nexus*, 3(2), p. pgae039.
49. Jung, H.S., Burgess, S.A., *et al.* (2008) 'Conservation of the regulated structure of folded myosin 2 in species separated by at least 600 million years of independent evolution', *Proceedings of the National Academy of Sciences*, 105(16), pp. 6022–6026.
50. Jung, H.S., Komatsu, S., *et al.* (2008) 'Head–Head and Head–Tail Interaction: A General Mechanism for Switching Off Myosin II Activity in Cells', *Molecular Biology of the Cell*, 19(8), pp. 3234–3242.
51. Jung, H.S. *et al.* (2011) 'Role of the Tail in the Regulated State of Myosin 2', *Journal of Molecular Biology*, 408(5), pp. 863–878.
52. Kampourakis, T. *et al.* (2014) 'Myosin binding protein-C activates thin filaments and inhibits thick filaments in heart muscle cells', *Proceedings of the National Academy of Sciences*, 111(52), pp. 18763–18768.
53. Kampourakis, T. and Irving, M. (2015) 'Phosphorylation of myosin regulatory light chain controls myosin head conformation in cardiac muscle', *Journal of Molecular and Cellular Cardiology*, 85, pp. 199–206.

54. Kawana, M. *et al.* (2017) 'Biophysical properties of human beta-cardiac myosin with converter mutations that cause hypertrophic cardiomyopathy.', *Science advances*, 3(2), p. e1601959.
55. Kawana, M. *et al.* (2023) 'Molecular characterization of a novel MYH7 mutation Q222H in a patient with severe dilated cardiomyopathy', *Biophysical Journal*, 122(3), p. 258a.
56. Kawana, M., Spudich, J.A. and Ruppel, K.M. (2022) 'Hypertrophic cardiomyopathy: Mutations to mechanisms to therapies', *Frontiers in Physiology*, 13, p. 975076.
57. Lee, K.H. *et al.* (2018) 'Interacting-heads motif has been conserved as a mechanism of myosin II inhibition since before the origin of animals', *Proceedings of the National Academy of Sciences of the United States of America*, 115(9), pp. E1991–E2000.
58. Lee, S. *et al.* (2024) 'Incomplete-penetrant hypertrophic cardiomyopathy *MYH7* G256E mutation causes hypercontractility and elevated mitochondrial respiration', *Proceedings of the National Academy of Sciences*, 121(19), p. e2318413121.
59. Lehman, S.J., Crocini, C. and Leinwand, L.A. (2022) 'Targeting the sarcomere in inherited cardiomyopathies', *Nature Reviews Cardiology*, 19(6), pp. 353–363.
60. Levine, R.J. *et al.* (1996) 'Myosin light chain phosphorylation affects the structure of rabbit skeletal muscle thick filaments', *Biophysical Journal*, 71(2), pp. 898–907.
61. Liu, J. *et al.* (2003) 'Refined Model of the 10S Conformation of Smooth Muscle Myosin by Cryo-electron Microscopy 3D Image Reconstruction', *Journal of Molecular Biology*, 329(5), pp. 963–972.
62. Liu, J. *et al.* (2006) 'Three-dimensional structure of the myosin V inhibited state by cryoelectron tomography', *Nature*, 442(7099), pp. 208–211.
63. Liu, L., Srikakulam, R. and Winkelmann, D.A. (2008) 'Unc45 activates Hsp90-dependent folding of the myosin motor domain.', *The Journal of biological chemistry*, 283(19), pp. 13185–93.
64. Lowey, S. and Trybus, K.M. (1995) 'Role of skeletal and smooth muscle myosin light chains.', *Biophysical journal*, 68(4 Suppl), pp. 120S-127S.
65. Lowey, S. and Trybus, K.M. (2010) 'Common Structural Motifs for the Regulation of Divergent Class II Myosins', *Journal of Biological Chemistry*, 285(22), pp. 16403–16407.
66. Ma, W. *et al.* (2023) 'Structural OFF/ON transitions of myosin in relaxed porcine myocardium predict calcium-activated force.', *Proceedings of the National Academy of Sciences of the United States of America*, 120(5), p. e2207615120.
67. Maron, M.S. *et al.* (2023) 'Phase 2 Study of Aficamten in Patients With Obstructive Hypertrophic Cardiomyopathy', *Journal of the American College of Cardiology*, 81(1), pp. 34–45.
68. Marston, S. *et al.* (2009) 'Evidence From Human Myectomy Samples That *MYBPC3* Mutations Cause Hypertrophic Cardiomyopathy Through Haploinsufficiency', *Circulation Research*, 105(3), pp. 219–222.
69. McNamara, J.W. *et al.* (2015) 'The role of super-relaxed myosin in skeletal and cardiac muscle.', *Biophysical reviews*, 7(1), pp. 5–14.
70. McNamara, J.W. *et al.* (2017) 'MYBPC3 mutations are associated with a reduced super-relaxed state in patients with hypertrophic cardiomyopathy.', *PloS one*, 12(6), p. e0180064.
71. Mohran, S. *et al.* (2024) 'The biochemically defined super relaxed state of myosin—A paradox', *Journal of Biological Chemistry*, 300(1), p. 105565.

72. Morck, M.M. *et al.* (2022) 'Hypertrophic cardiomyopathy mutations in the pliant and light chain-binding regions of the lever arm of human β-cardiac myosin have divergent effects on myosin function', *eLife*, 11, p. e76805.
73. Moss, R.L., Fitzsimons, D.P. and Ralphe, J.C. (2015) 'Cardiac MyBP-C regulates the rate and force of contraction in mammalian myocardium', *Circulation research*, 116(1), pp. 183–192.
74. Mun, J.Y. *et al.* (2014) 'Myosin-binding protein C displaces tropomyosin to activate cardiac thin filaments and governs their speed by an independent mechanism', *Proceedings of the National Academy of Sciences of the United States of America*, 111(6), pp. 2170–2175.
75. Naber, N., Cooke, R. and Pate, E. (2011) 'Slow myosin ATP turnover in the super-relaxed state in tarantula muscle', *Journal of Molecular Biology*, 411(5), pp. 943–950.
76. Nag, S. *et al.* (2015) 'Contractility parameters of human beta-cardiac myosin with the hypertrophic cardiomyopathy mutation R403Q show loss of motor function.', *Science advances*, 1(9), p. e1500511.
77. Nag, S. *et al.* (2017) 'The myosin mesa and the basis of hypercontractility caused by hypertrophic cardiomyopathy mutations.', *Nature structural & molecular biology*, 24(6), pp. 525–533.
78. Nag, S. *et al.* (2023) 'Mavacamten, a precision medicine for hypertrophic cardiomyopathy: From a motor protein to patients', *Science Advances*, 9(30), p. eabo7622.
79. Nandwani, N. *et al.* (2024) 'Hypertrophic cardiomyopathy mutations Y115H and E497D disrupt the folded-back state of human β-cardiac myosin allosterically', *bioRxiv*, p. 2024.02.29.582851.
80. Nelson, S. *et al.* (2023) 'Myosin-binding protein C stabilizes, but is not the sole determinant of SRX myosin in cardiac muscle', *Journal of General Physiology*, 155(4), p. e202213276.
81. Oakley, C.E. *et al.* (2007) 'Myosin binding protein—C: Enigmatic regulator of cardiac contraction', *The International Journal of Biochemistry & Cell Biology*, 39(12), pp. 2161–2166.
82. Offer, G. and Knight, P. (1996) 'The Structure of the Head-Tail Junction of the Myosin Molecule', *Journal of Molecular Biology*, 256(3), pp. 407–416.
83. Padrón, R. *et al.* (1991) 'X-ray diffraction study of the structural changes accompanying phosphorylation of tarantula muscle', *Journal of Muscle Research and Cell Motility*, 12(3), pp. 235–241.
84. Pfuhl, M. and Gautel, M. (2012) 'Structure, interactions and function of the N-terminus of cardiac myosin binding protein C (MyBP-C): who does what, with what, and to whom?', *Journal of muscle research and cell motility*, 33(1), pp. 83–94.
85. Pilagov, M. *et al.* (2023) 'Single-molecule imaging reveals how mavacamten and PKA modulate ATP turnover in skeletal muscle myofibrils', *Journal of General Physiology*, 155(1), p. e202213087.
86. Previs, M.J. *et al.* (2012) 'Molecular Mechanics of Cardiac Myosin-Binding Protein C in Native Thick Filaments', *Science*, 337(6099), pp. 1215–1218.
87. Previs, M.J., Michalek, A.J. and Warshaw, D.M. (2014) 'Molecular modulation of actomyosin function by cardiac myosin-binding protein C', *Pflügers Archiv - European Journal of Physiology*, 466(3), pp. 439–444.

88. Rahmani, H. *et al.* (2021) 'The myosin II coiled-coil domain atomic structure in its native environment', *Proceedings of the National Academy of Sciences*, 118(14), p. e2024151118.
89. Rahmanseresht, S. *et al.* (2021) 'The N terminus of myosin-binding protein C extends toward actin filaments in intact cardiac muscle', *Journal of General Physiology*, 153(3), p. e202012726.
90. Rasicci, D. V *et al.* (2022) 'Dilated cardiomyopathy mutation E525K in human beta-cardiac myosin stabilizes the interacting-heads motif and super-relaxed state of myosin.', *eLife*, 11:e77415.
91. Ratti, J. *et al.* (2011) 'Structure and interactions of myosin-binding protein C domain C0: cardiac-specific regulation of myosin at its neck?', *The Journal of biological chemistry*, 286(14), pp. 12650–12658.
92. Resnicow, D.I. *et al.* (2010) 'Functional diversity among a family of human skeletal muscle myosin motors', *Proceedings of the National Academy of Sciences*, 107(3), pp. 1053–1058.
93. Robert-Paganin, J., Auguin, D. and Houdusse, A. (2018) 'Hypertrophic cardiomyopathy disease results from disparate impairments of cardiac myosin function and auto-inhibition', *Nature communications*, 9(1), p. 4019.
94. Vander Roest, A.S. *et al.* (2021) 'Hypertrophic cardiomyopathy β-cardiac myosin mutation (P710R) leads to hypercontractility by disrupting super relaxed state.', *Proceedings of the National Academy of Sciences of the United States of America*, 118(24), p. e2025030118.
95. Rohde, J.A. *et al.* (2018) 'Mavacamten stabilizes an autoinhibited state of two-headed cardiac myosin', *Proceedings of the National Academy of Sciences*, 115(32), pp. E7486-E7494.
96. Saberi, S. *et al.* (2021) 'Mavacamten Favorably Impacts Cardiac Structure in Obstructive Hypertrophic Cardiomyopathy', *Circulation*, 143(6), pp. 606–608.
97. Sarkar, S.S. *et al.* (2020) 'The hypertrophic cardiomyopathy mutations R403Q and R663H increase the number of myosin heads available to interact with actin.', *Science advances*, 6(14), p. eaax0069.
98. Scarff, C.A. *et al.* (2020) 'Structure of the shutdown state of myosin-2', *Nature*, 588(7838), pp. 515–520.
99. Scruggs, S.B. and Solaro, R.J. (2011) 'The significance of regulatory light chain phosphorylation in cardiac physiology', *Archives of Biochemistry and Biophysics*, 510(2), pp. 129–134.
100. Seidman, J.G. and Seidman, C. (2001) 'The Genetic Basis for Cardiomyopathy', *Cell*, 104(4), pp. 557–567.
101. Semsarian, C. *et al.* (2015) 'New perspectives on the prevalence of hypertrophic cardiomyopathy', *Journal of the American College of Cardiology*, 65(12), pp. 1249–1254.
102. Sen-Martín, L. *et al.* (2024) 'Broad therapeutic benefit of myosin inhibition in hypertrophic cardiomyopathy', *bioRxiv*, p. 2024.03.22.584986.
103. Singh, R.R., McNamara, J.W. and Sadayappan, S. (2021) 'Mutations in myosin S2 alter cardiac myosin-binding protein-C interaction in hypertrophic cardiomyopathy in a phosphorylation-dependent manner.', *The Journal of biological chemistry*, 297(1), p. 100836.
104. Sommese, R.F. *et al.* (2013) 'Molecular consequences of the R453C hypertrophic cardiomyopathy mutation on human β-cardiac myosin motor function', *Proceedings of the National Academy of Sciences of the United States of America*, 110(31), pp. 12607–12612.

105. Spudich, J.A. (2015) 'The myosin mesa and a possible unifying hypothesis for the molecular basis of human hypertrophic cardiomyopathy.', *Biochemical Society transactions*, 43(1), pp. 64–72.
106. Spudich, J.A. *et al.* (2016) 'Effects of hypertrophic and dilated cardiomyopathy mutations on power output by human beta-cardiac myosin.', *The Journal of experimental biology*, 219(Pt 2), pp. 161–167.
107. Spudich, J.A. (2019) 'Three perspectives on the molecular basis of hypercontractility caused by hypertrophic cardiomyopathy mutations.', *Pflugers Archiv : European journal of physiology*, 471(5), pp. 701–717.
108. Srikakulam, R. and Winkelmann, D.A. (2004) 'Chaperone-mediated folding and assembly of myosin in striated muscle.', *Journal of cell science*, 117(Pt 4), pp. 641–52.
109. Stewart, M.A. *et al.* (2010) 'Myosin ATP turnover rate is a mechanism involved in thermogenesis in resting skeletal muscle fibers.', *Proceedings of the National Academy of Sciences of the United States of America*, 107(1), pp. 430–5.
110. Sulbarán, G. *et al.* (2015) 'An invertebrate smooth muscle with striated muscle myosin filaments', *Proceedings of the National Academy of Sciences*, 112(42), pp. E5660-E5668.
111. Tama, F. *et al.* (2005) 'The Requirement for Mechanical Coupling Between Head and S2 Domains in Smooth Muscle Myosin ATPase Regulation and its Implications for Dimeric Motor Function', *Journal of Molecular Biology*, 345(4), pp. 837–854.
112. Tamborrini, D. *et al.* (2023) 'Structure of the native myosin filament in the relaxed cardiac sarcomere', *Nature*, 623(7988), pp. 863–871.
113. Toepfer, C. *et al.* (2013) 'Myosin Regulatory Light Chain (RLC) Phosphorylation Change as a Modulator of Cardiac Muscle Contraction in Disease', *Journal of Biological Chemistry*, 288(19), pp. 13446–13454.
114. Toepfer, C.N. *et al.* (2019) 'Hypertrophic cardiomyopathy mutations in MYBPC3 dysregulate myosin.', *Science translational medicine*, 11(476), p. eaat1199.
115. Toepfer, C.N. *et al.* (2020) 'Myosin Sequestration Regulates Sarcomere Function, Cardiomyocyte Energetics, and Metabolism, Informing the Pathogenesis of Hypertrophic Cardiomyopathy', *Circulation*, pp. 828–842.
116. Trivedi, D. V *et al.* (2018) 'Hypertrophic cardiomyopathy and the myosin mesa: viewing an old disease in a new light.', *Biophysical reviews*, 10(1), pp. 27–48.
117. Trybus, K.M. *et al.* (1997) 'Spare the rod, spoil the regulation: necessity for a myosin rod.', *Proceedings of the National Academy of Sciences of the United States of America*, 94(1), pp. 48–52.
118. Trybus, K.M., Huiatt, T.W. and Lowey, S. (1982) 'A bent monomeric conformation of myosin from smooth muscle.', *Proceedings of the National Academy of Sciences*, 79(20), pp. 6151–6155.
119. Trybus, K.M. and Lowey, S. (1984) 'Conformational states of smooth muscle myosin. Effects of light chain phosphorylation and ionic strength.', *The Journal of biological chemistry*, 259(13), pp. 8564–71.
120. Vandenboom, R. (2016) 'Modulation of Skeletal Muscle Contraction by Myosin Phosphorylation', in *Comprehensive Physiology*. Wiley, pp. 171–212.

121. Vera, C.D. *et al.* (2019) 'Myosin motor domains carrying mutations implicated in early or late onset hypertrophic cardiomyopathy have similar properties', *Journal of Biological Chemistry*, 294(46), pp. 17451–17462.
122. Virani, S.S. *et al.* (2020) 'Heart Disease and Stroke Statistics—2020 Update: A Report From the American Heart Association', *Circulation*, 141(9), pp. e139-e596.
123. Walklate, J. *et al.* (2022) 'Exploring the super-relaxed state of myosin in myofibrils from fast-twitch, slow-twitch, and cardiac muscle.', *The Journal of biological chemistry*, 298(3), p. 101640.
124. Wang, J. *et al.* (2014) 'Malignant effects of multiple rare variants in sarcomere genes on the prognosis of patients with hypertrophic cardiomyopathy', *European Journal of Heart Failure*, 16(9), pp. 950–957.
125. Wendt, T. *et al.* (1999) 'Visualization of Head–Head Interactions in the Inhibited State of Smooth Muscle Myosin', *The Journal of Cell Biology*, 147(7), pp. 1385–1390.
126. Wendt, T. *et al.* (2001) 'Three-dimensional image reconstruction of dephosphorylated smooth muscle heavy meromyosin reveals asymmetry in the interaction between myosin heads and placement of subfragment 2', *Proceedings of the National Academy of Sciences*, 98(8), pp. 4361–4366.
127. Woodhead, J.L. *et al.* (2005) 'Atomic model of a myosin filament in the relaxed state', *Nature*, 436(7054), pp. 1195–1199.
128. Woodhead, J.L., Zhao, F.-Q. and Craig, R. (2013) 'Structural basis of the relaxed state of a Ca2+-regulated myosin filament and its evolutionary implications.', *Proceedings of the National Academy of Sciences of the United States of America*, 110(21), pp. 8561–8566.
129. Yang, S. *et al.* (2020) 'Cryo-EM structure of the inhibited (10S) form of myosin II', *Nature*, 588(7838), pp. 521–525.
130. Yuan, C.C. *et al.* (2022) 'Molecular basis of force-pCa relation in MYL2 cardiomyopathy mice: Role of the super-relaxed state of myosin', *Proceedings of the National Academy of Sciences of the United States of America*, 119(8), p. e2110328119.
131. Zhao, F.-Q., Craig, R. and Woodhead, J.L. (2009) 'Head–Head Interaction Characterizes the Relaxed State of Limulus Muscle Myosin Filaments', *Journal of Molecular Biology*, 385(2), pp. 423–431.
132. Zoghbi, M.E. *et al.* (2008) 'Three-dimensional structure of vertebrate cardiac muscle myosin filaments', *Proceedings of the National Academy of Sciences*, 105(7), pp. 2386–2390.

Figure 1

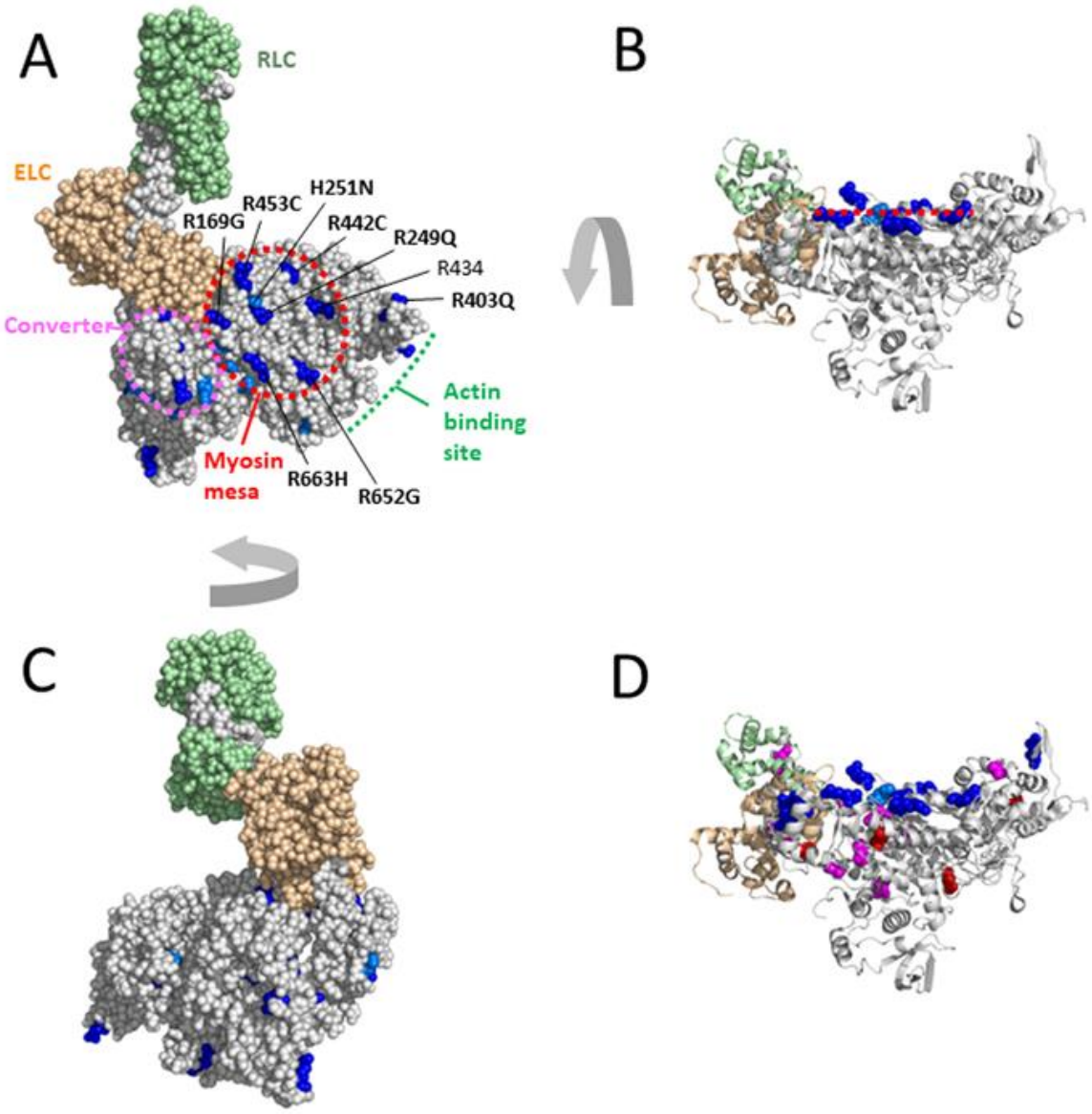
A
RLC
ELC
R453C
H251N
R169G
R442C
R249Q
R434
R403Q
Converter
Actin
binding
site
Myosin
mesa
R663H
R652G
B
C
D

Figure 2

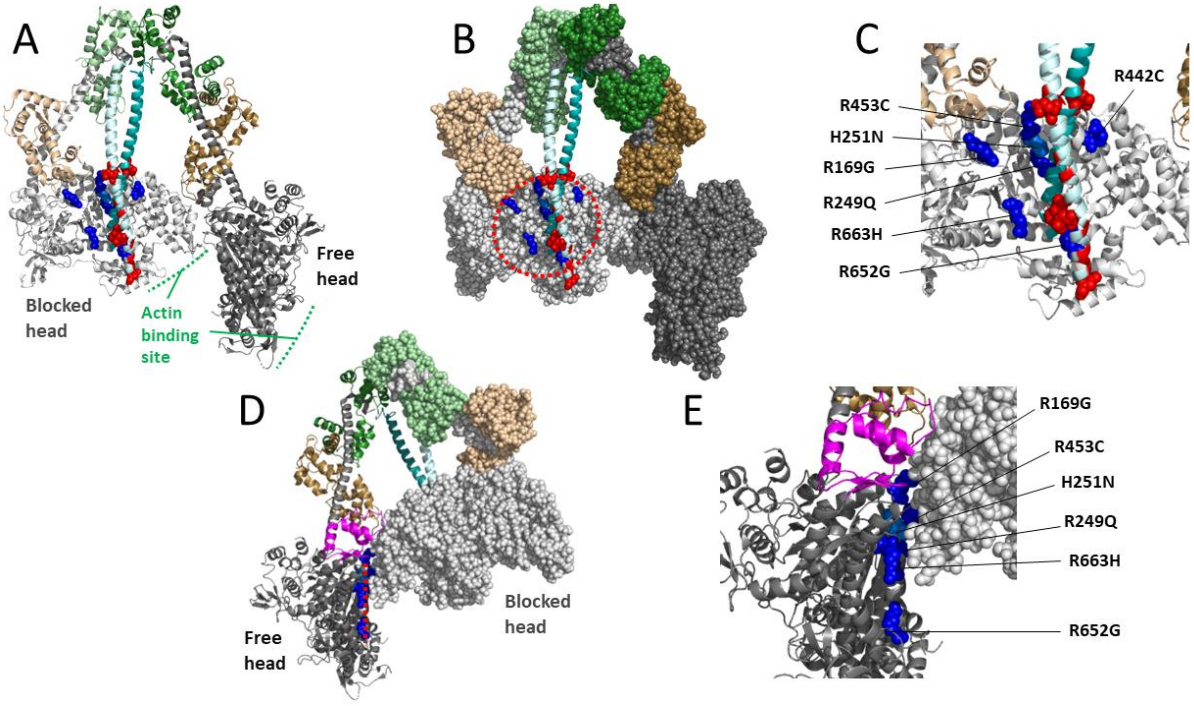

Figure 3

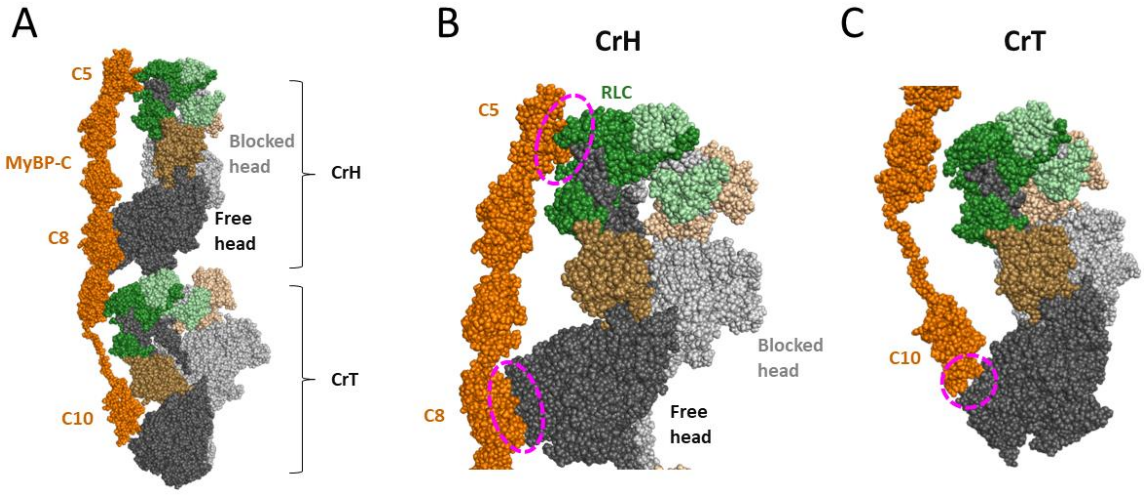

Figure 4

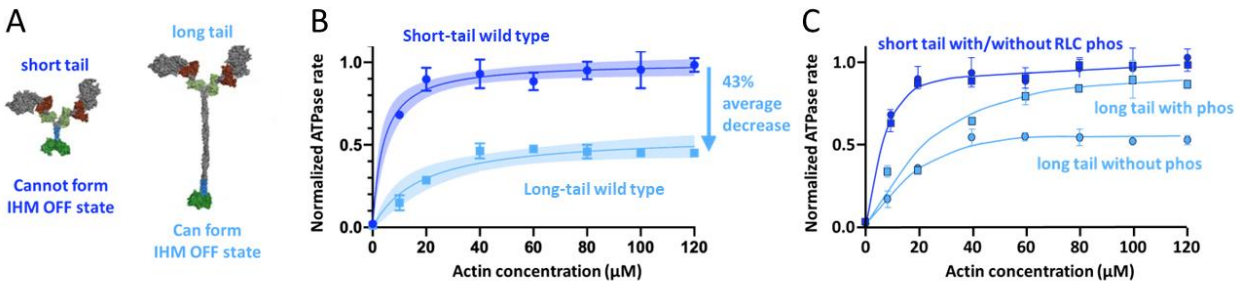

Figure 5

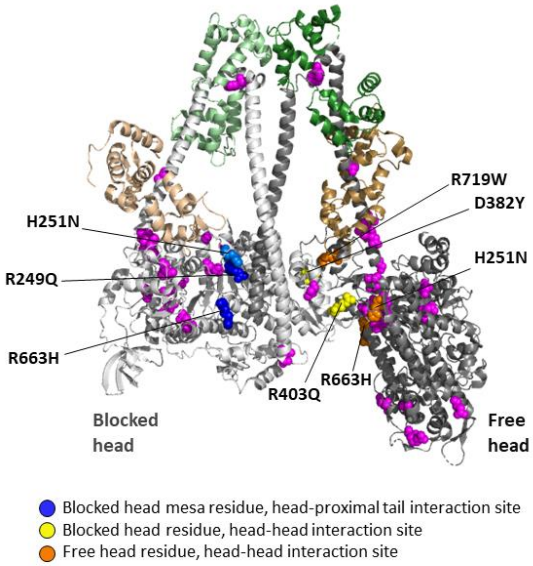

Figure 6

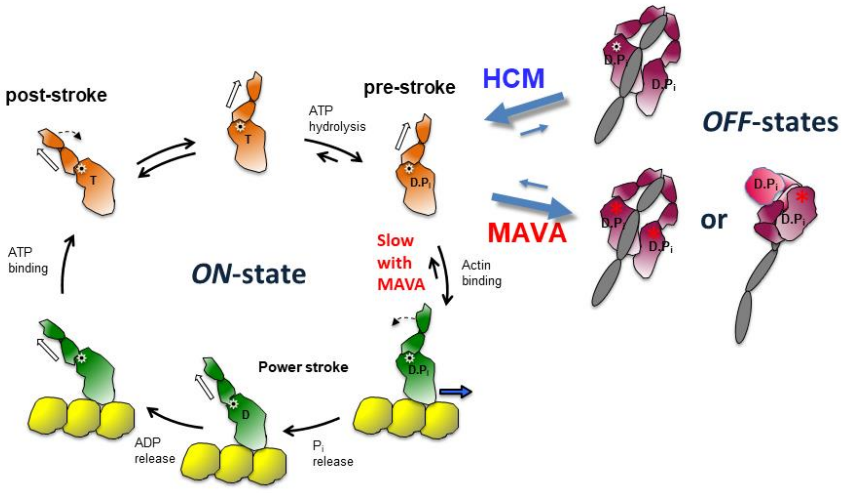

Figure 7

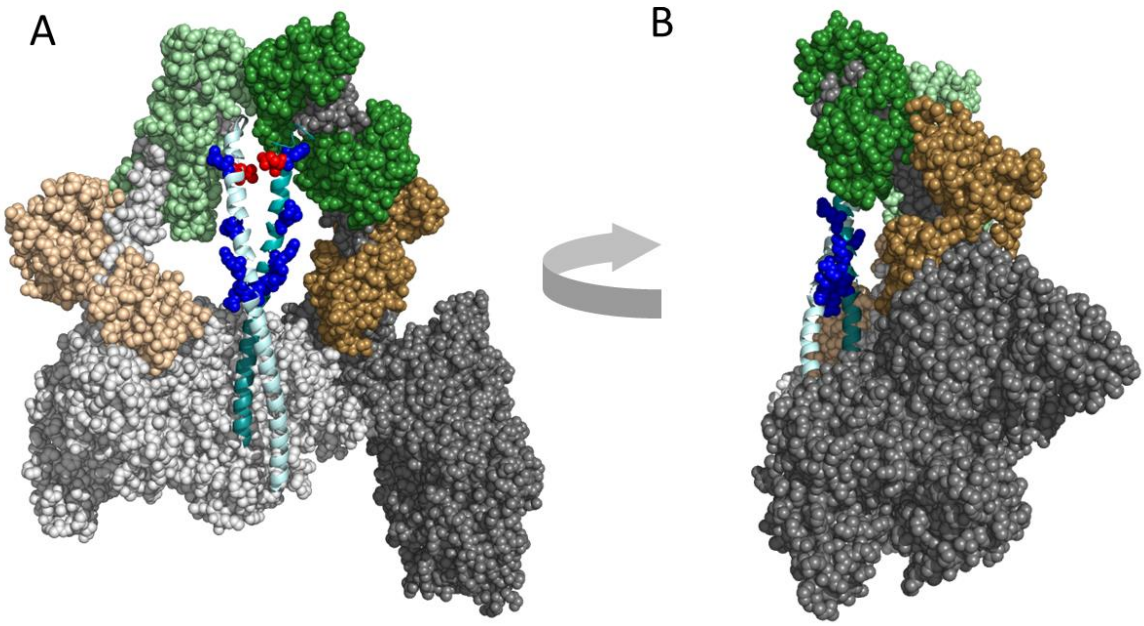

Table 1

HCM mutation	Actin-activated ATPase k_{cat} % increase % decrease	Motility velocity % increase % decrease	Intrinsic force % increase % decrease	Decrease in SRX (%)	Increase in additional N_a by LSAR assay (%)	References
Y115H	0	45		82	80	(Nandwani *et al.*, 2024)
Q222K	30	32		49	100	Kawana *et al.*, unpublished results
D239N	50	95	23			(Adhikari *et al.*, 2016)
R249Q *	30			64	91	(Adhikari *et al.*, 2019)
H251N *‡	24	40	45	36	79	(Adhikari *et al.*, 2016, 2019)
G256E	0	20		45	53	(Lee *et al.*, 2023)
D382Y †	20	10		45	63	(Vera *et al.*, 2019; Adhikari *et al.*, 2019)
R403Q †	25	15	15	64	58	(Nag *et al.*, 2015; Sarkar *et al.*, 2020)
R453C	30	25	50			(Sommese *et al.*, 2013)
I457T	75	240		0	0	(Adhikari *et al.*, 2019)
E497D	50	20		82	80	(Nandwani *et al.*, 2024)
E536D	0	0		0	50	Nandwani *et al.*, unpublished results
V606M	75	60		0	77	Nandwani *et al.*, unpublished results
R663H *‡	0	0	0	67	26	(Sarkar *et al.*, 2020)
P710R	40	50		54	88	(Vera *et al.*, 2019; Vander Roest *et al.* 2021)
R719W ‡	0	0	15	64	100	(Kawana *et al.*, 2017; Adhikari *et al.*, 2019)
G741R	0	0	0			(Kawana *et al.*, 2017)
G768R	30	80		0	63	Pathak *et al.*, unpublished results
D778V	15	46		0	56	(Morck *et al.*, 2022)
L781P	0	30		0	65	(Morck *et al.*, 2022)
S782N	0	0		0	56	(Morck *et al.*, 2022)
A797T	0	5		54	100	(Morck *et al.*, 2022)
F834L	0	0		64	58	(Morck *et al.*, 2022)

* Blocked head mesa residue, head-proximal tail interaction site
† Blocked head residue, head-head interaction site
‡ Free head residue, head-head interaction site

Table 2

Gene	HCM mutation	Sample type	Decrease in SRX (%)	Notes	References
MYH7	R403Q	iPSC-CM	~10*	SRX destabilization seen with purified proteins (Sarkar *et al.*, 2020)	(Toepfer *et al.*, 2020)
	V606M	iPSC-CM	~10*	SRX destabilization not seen with purified proteins (Nandwani *et al.*, unpublished results)	(Toepfer *et al.*, 2020)
	R663H	human cardiac tissue	28	SRX destabilization seen with purified proteins (Sarkar *et al.*, 2020)	(Anderson *et al.*, 2018)
	R719W	iPSC-CM	~14*	SRX destabilization seen with purified proteins (Adhikari *et al.*, 2019)	(Toepfer *et al.*, 2020)
MYBPC3	V365E, E542Q	human cardiac tissue	38	HCM patient with two *MYBPC3* mutations	(McNamara *et al.*, 2017)
	E461X	human cardiac tissue	31		(McNamara *et al.*, 2017)
	L527 fs/3	human cardiac tissue	33		(McNamara *et al.*, 2017)
	D770N, E143K (*MYL3*)	human cardiac tissue	50	HCM patient with *MYBPC3* and *MYL3* (essential light chain) mutations	(McNamara *et al.*, 2017)
	$MYBPC3_{mut}$	human cardiac tissue	23#	Data combined from 3 HCM patients with distinct heterozygous frameshift truncating variants Gln981fs, Leu1014fs, and Lys1209fs	(Toepfer *et al.*, 2019)